Journal of Metals, Materials and Minerals, Vol. 30, No. 4, pp. 90-96, 2020

Ultraviolet-shielding and water resistance properties of graphene quantum dots/ polyvinyl alcohol composite-based film

Sutthipoj WONGRERKDEE[1] and Pichitchai PIMPANG[2,*]

[1] *Department of Physics, Faculty of Liberal Arts and Science, Kasetsart University Kamphaeng Saen Campus, Nakhon Pathom 73140, Thailand*

[2] *Faculty of Science and Technology, Pibulsongkram Rajabhat University, Phitsanulok 65000, Thailand*

***Corresponding author e-mail:** p.pimpang@psru.ac.th

Received date:
4 January 2020
Revised date
29 June 2020
Accepted date:
11 August 2020

Keywords:
Graphene quantum dots;
UV-shielding;
Optical transmittance;
UV absorption;
Water resistance

Abstract

The Ultraviolet-shielding (UV-shielding) and water resistance properties of graphene quantum dots/polyvinyl alcohol (GQDs/PVA) composite-based film have been investigated. The GQDs/PVA composite-based films were fabricated with different GQDs concentrations of 0, 5, 10, 15, and 20 wt%. The optical property of GQDs was carried out by utilizing fluorescence spectroscopy. Characterizations of GQDs/PVA composite-based films were performed by using FT-IR spectroscopy, and UV-vis spectroscopy. It was found that GQDs exhibited the strongest excitation wavelength in the UV range. GQDs/PVA composite-based films offered an improved UV-shielding capacity when compared to PVA films and glass. Particularly, the GQDs/PVA composite-based film containing 20 wt% GQDs exhibited a UV transmittance of 9.8%, combined with 84% optical transparency. For humidity environment application, the highest contact angle was explored for the 10 wt% GQDs contents suggesting sustainability for humidity environment application. Accordingly, GQDs played an important role in UV-shielding by considering the effect of UV absorption of GQDs and the UV absorption of GQDs can be explained in terms of the photon excitation by UV light. This GQDs/PVA composite could be potentially applied as transparent UV-protective coatings for pharmaceutical packing, food products packing, and UV-shielding or UV filter glass.

1. Introduction

Present, the serious acute and chronic health effects caused by terrestrial solar ultraviolet (UV) radiation that directly radiates from the sun are in critical condition since the risk of direct contact with UV is high. The wavelength of UV spectra is further subdivided into UVA (320-400 nm), UVB (280-320 nm) and UVC (100-280 nm) [1,2]. Normally, the spectra of terrestrial solar UV radiation reach the Earth's surface is ~295-400 nm [1]. UVC has no irradiation to the Earth because it is completely absorbed by stratospheric ozone. UVB accounts for less than 5% of terrestrial solar UV radiation, whereas it has high intensity at around midday [2]. Accordingly, UVA is the main component of terrestrial solar UV radiation, which remains fairly consistent throughout the day. It is well-known that the main cause of the sun's damaging effects on the skin is the risk of harmful involving sunburn [2] and the risk factor of skin cancer [3,4] and the acceleration of skin aging [3]. Additionally, Photodegradation of foods, beverages, and pharmaceuticals that is sensitive to UV light can lead to structural changes [5,6]. Hence, research and development of UV protection are necessary.

Graphene and graphene-based nanomaterials (i.e., graphene oxide, reduced graphene oxide, and graphene quantum dots) have a large number of applications such as photonic [7], optoelectronic [8], and UV filters [9,10], which benefit from a characteristic absorption in UV region [11-14]. Among them, a graphene quantum dot (GQDs) is a promising material for UV-shielding films because of its strong absorption spectrum in UV region [12], size-dependent optical properties [12], almost transparent to visible light [15], rapid synthesis via carbonization of citric acid precursor [12], and tunable photoluminescence colors on changing band gap via different synthesis conditions [16]. In addition, GQDs/polymer-based UV-shielding films may have advantageous mechanical properties due to flexibility and without the crystal structure distortion of the GQDs in the film. In example, UV-shielding property of silan-functionized graphene quantum dot nanofluids (SiGQDs) gel glasses has been reported previously [17]. SiGQDs gel glasses are able to block the UV from 190 to 400 nm in all wavelengths, meanwhile high transparency in the visible region is still obtained. However, Polyvinyl alcohol is a candidate because it has a wide variety of potential applications, especially for packaging [18-20]. Therefore, GQDs/Polyvinyl alcohol-based film was also a promising material for UV protection packaging (i.e., food and pharmaceutical bags).

In this work, the Ultraviolet-shielding (UV-shielding) property of graphene quantum dots/polyvinyl alcohol (GQDs/PVA) composite-based film was investigated. GQDs/PVA composite-based films were prepared by screen printing of GQDs/PVA composite gel on the glass substrate and characterized using several techniques including preliminary optical test, fluorescence spectroscopy, Fourier transform

infrared spectroscopy (FT-IR), ultraviolet-visible (UV-vis) spectroscopy, and contact angle measurement. GQDs/PVA composite gel was prepared by adding GQDs in PVA at different concentrations of 0, 5, 10, 15, and 20 wt%. PVA is a promising candidate because it is highly transparent [21] and water solubility [22]. These hydroxyl groups (OH) of PVA are a source of hydrogen bonding [23] and hence assist the formation of polymer composite by growing nano-sized materials inside polymer matrixes. GQDs are a good candidate for UV-shielding applications because it meets a commercial ultraviolet filter requirement of broad absorption in the UV region. According to previous reports, GQDs is high solubility in polar solvents such as ethanol [12], and water [8,24]. Therefore, hydroxyl groups and carboxyl groups that functionalized onto crystalline GQDs [12] may be served hydrogen bonding on PVA chains.

2. Experimental

A schematic diagram of the GQDs/PVA composite-based film preparation is shown in Figure 1.

The GQDs were prepared by tuning the carbonization degree of the citric acid precursor as described in the previous report [12]. Briefly, 1.0 M of citric acid precursor (CA) was first prepared by dissolving 52.535 g of citric acid (monohydrate) powder (99.5%, Loba Chemie; MW 210.14 g·mol^{-1}) in 250 ml of ethanol (99.5%, Merck). Then, a pyrex beaker was heated at a constant temperature of 250°C using a hot plate stirrer (IKA C-MAG HS7). After that, the CA solution was added dropwise into a heated beaker to maintain the temperature. According to the heating CA solution, the CA solution changed from an initial colorless solution to melted yellow. Finally, the synthesized GQDs were stored at room temperature. To prepared UV-shielding films, a transparent PVA gel was first prepared by dissolving 15 g of polyvinyl alcohol powder (Fluka; MW~67,000 g·mol^{-1}) in 85 g of distilled water. Then, the GQDs was added into a transparent PVA gel at different concentrations of 0, 5, 10, 15, and 20 wt%, and stirred at room temperature until a light yellow of GQDs/PVA composite gel was formed. Next, UV/ozone treatment was used to clean the surface of glass substrates. After that, the GQDs/PVA composite gel was coated on a glass substrate using a screen-printing technique. In all cases, the film thickness of approximately 60 µm was controlled by using one layer of tap spacer (3M magic tape 810). Finally, GQDs/PVA composite coated on glass substrates were sintered at 120°C overnight to form the GQDs/PVA composite-based films.

Optical properties of the GQDs were analyzed by fluorescence spectroscopy (ShimadzuRF-6000). Excitation-emission contour maps of the GQDs were performed by utilizing excitation wavelength in the range of 300-500 nm. Fourier transform infrared (FT-IR) spectroscopy (Thermo scientific NicoletTMiS) was carried out on the surface of GQDs, PVA, and GQDs/PVA composite to identify the material's molecular composition and structure. FT-IR spectra were observed in the range of 500-4000 cm^{-1}. Optical properties of UV-shielding films were obtained by UV-vis spectroscopy (Shimadzu UV-2450). Transmittance spectra of UV-shielding films were recorded in the range of 300-900 nm. Contact angle measurement was carried out for 60 s under a small drop (15 µL) of water.

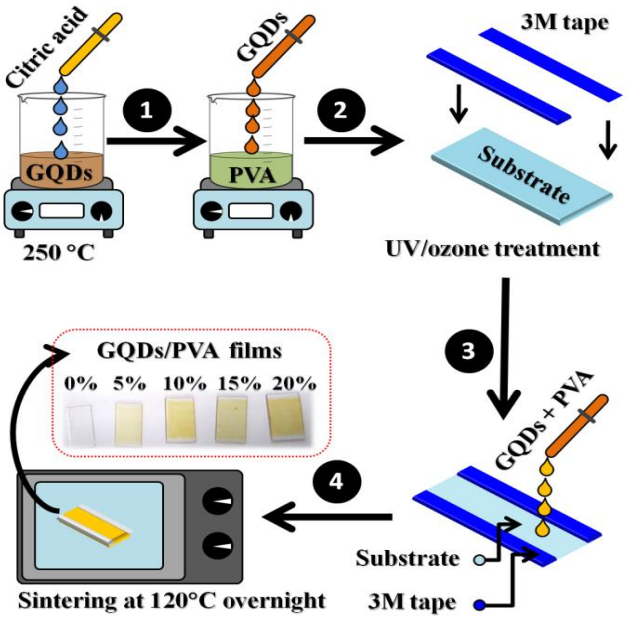

Figure 1. A schematic diagram of UV-shielding films preparation.

3. Results and discussion

Figure 2 shows a simple test for the optical transmittance of the GQDs solution. The optical transmittance was observed by irradiating three different colors of laser pointers to the GQDs solution. The GQDs solution was obtained by adding ethanol into the synthesized GQDs to maintain initial volume and stored in a clear bottle. Based on observation by naked eyes, the GQDs solution had a high transmittance for under irradiation of the green and red lasers excepted for under the purple laser irradiation (wavelength at 405±10 nm) in which without a transmittance. This result suggested that the GQDs solution could be absorbed near UVA light such as purple but could not be absorbed visible light (i.e., green and red).

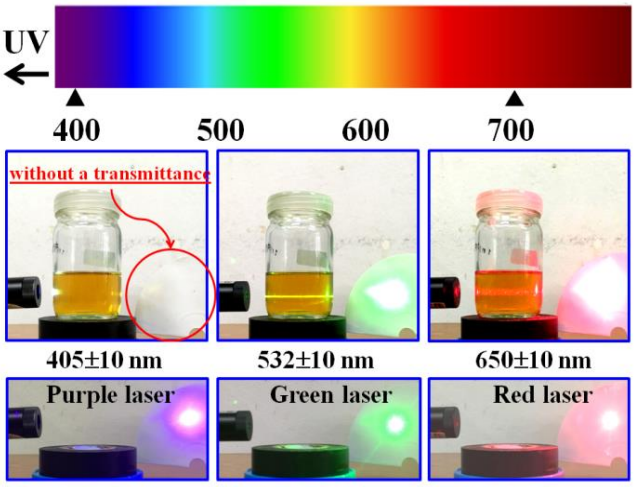

Figure 2. Simple test for the optical transmittance of the GQDs solution. The optical transmittance was observed under purple, green and red laser irradiation that has wavelength at 405±10, 532±10, and 650±10 nm, respectively.

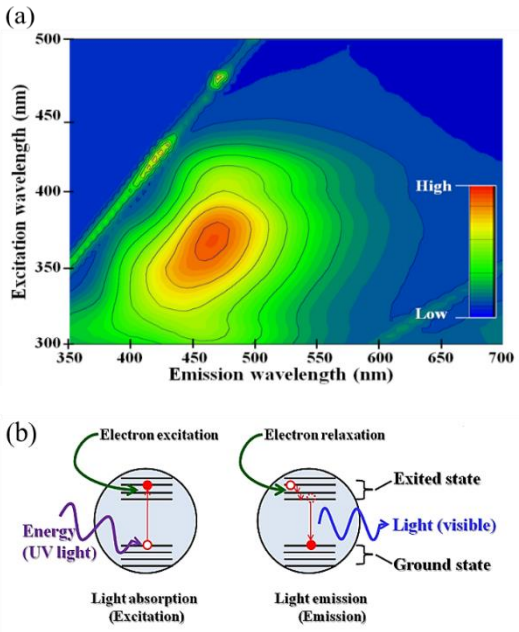

Figure 3. Excitation–emission contour map of the GQDs prepared at 250°C using 1.0 M of citric acid (a), and a schematic diagram for light-absorption/emission of the GQDs (b).

To determine the characteristics of the GQDs, the excitation-emission contour map of the GQDs was observed using fluorescence spectroscopy and is shown in Figure 3(a). The emission wavelengths from 350 nm to 700 nm can be achieved with the variation of the excitation wavelength in steps of 1 nm from 300 to 500 nm. The bright area of the excitation wavelength (y-axis) corresponds to high excitation intensity, which was directly related to light absorption in the GQDs. The bright area of the emission wavelength (x-axis) corresponds to high emission intensity, which was due to photo-emission by the GQDs. It was found that the GQDs exhibited the strongest excitation wavelength in the range of 320-400 nm and the strongest emission wavelength in the range of 442-497 nm. Thus, this result indicated that the GQDs had potentially UV absorption. The schematic diagram for the light-absorption/emission of the GQDs is proposed in Figure 3(b).

When the GQDs absorbed light (hence energy), electrons were raised from the ground state to the excited state. Then, electrons return to the ground state with a variety of transitions which may involve the emission of light. This effect is termed fluorescence. The emitted light will always be longer wavelength than the exciting light because the feature of quantum dots is the photoluminescence red-shift relative to absorption [25-27], also called the Stokes shift [28]. The energy may also be lost by non-radiative processes (electron relaxation), and eventually dissipated as heat.

Figure 4 indicates the FT-IR spectra of the GQDs, PVA, and GQDs/PVA composite. FT-IR spectra of the GQDs/PVA composite containing 5 wt% GQDs was demonstrated to represent the material's molecular composition and structure for GQDs/PVA composites that prepared using 10, 15, and 20 wt% of GQDs in PVA because all vibration modes were quite similar. FT-IR spectra of the GQDs (Figure 4(a)) showed the C–H stretching at 2985 cm^{-1}, the C=O stretching at 1706 cm^{-1}, the –OH band at 1374 cm^{-1} [29], the C–OH stretching at 1181 cm^{-1}, and the C–O stretching at 1020 cm^{-1}, implying the vibration of hydroxyl group (OH) and carboxyl group (COOH) that functionalized onto crystalline GQDs [11,12]. A FT-IR spectrum of gaseous CO_2 in a porous structure was detected at 2360 cm^{-1}. FT-IR spectra of the PVA (Figure 4(b)) showed the OH stretching at 3282 cm^{-1}, the CH_2 asymmetric stretching at 2940 cm^{-1}, the C–H bending of CH_2 at 1420 cm^{-1}, the OH rocking with CH wagging at 1324 cm^{-1}, and OH bending and the C–O stretching of acetyl groups at 1085 cm^{-1}, and the C–C stretching at 842 cm^{-1}, identifying molecular composition of PVA [30]. Figure 4(c) shows that peak intensities of the GQDs/PVA composite were decreased in all vibrations, which could be an effect of the feature of GQDs/PVA composite's solid. Obviously, the OH stretching at 3282 cm^{-1} of PVA shifted toward lower wavenumber to 3267 cm^{-1}. This is in good agreement with a previous report [31-35] that a shifted toward lower wavenumber of PVA indicating hydrogen bond formation between PVA molecule and polar materials. In addition, FT-IR spectra of the GQDs/PVA composite exhibited a decrease in intensity of -OH groups also indicating hydrogen bond formation between PVA molecule and the polar surface of GQDs. Thus, this result also suggested the hydrogen bond formation between PVA chains and GQDs [36] because the active COOH and OH groups that functionalized onto crystalline GQDs could be served physical cross-linking points on PVA chains via the hydrogen bonding.

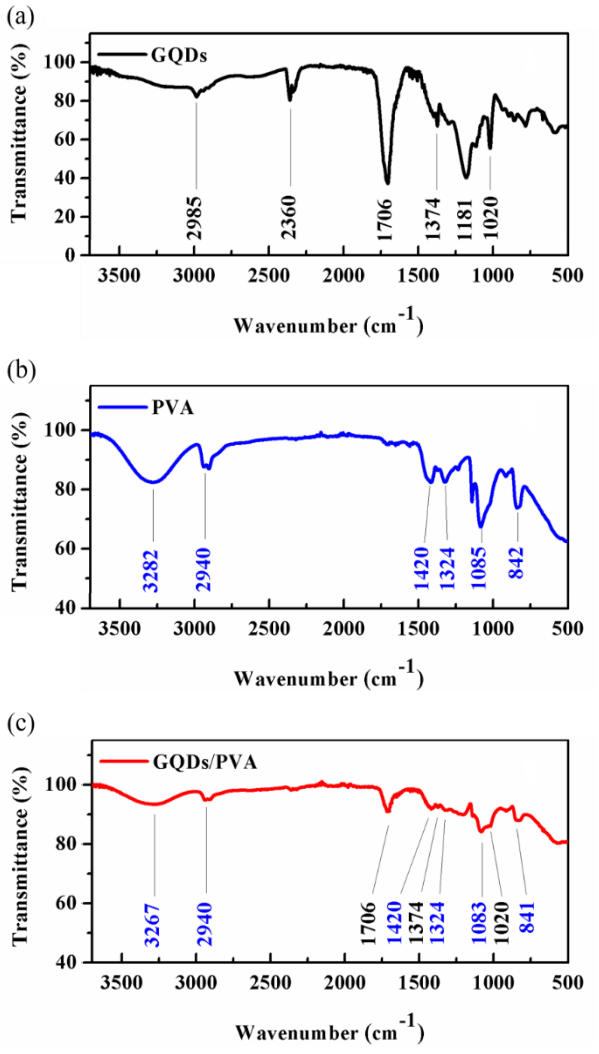

Figure 4. FT-IR spectra of the GQDs (a), PVA (b), and the GQDs/PVA composite containing 5 wt% GQDs (c).

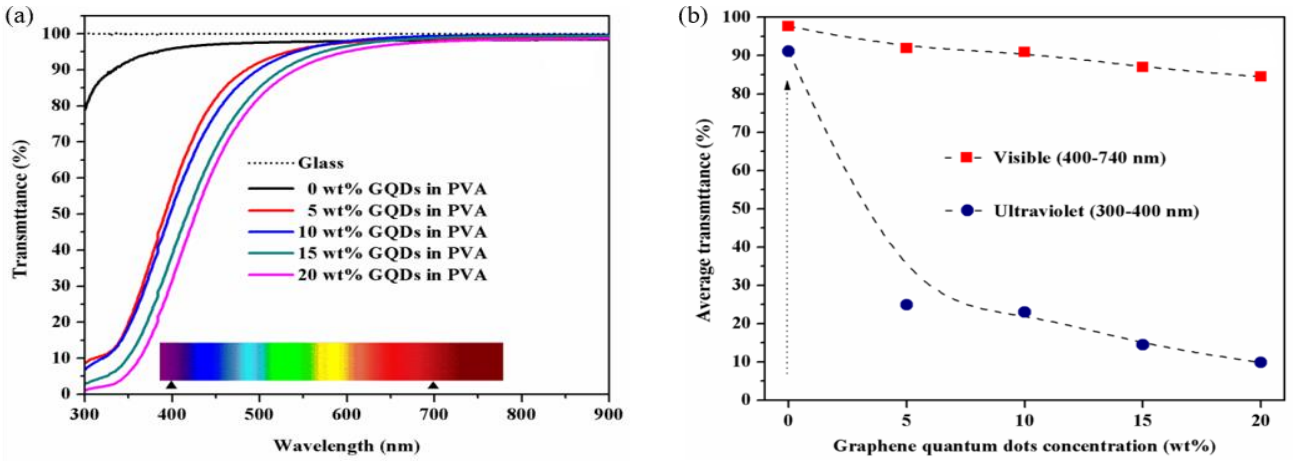

Figure 5. UV-vis transmittance spectra (a), and average transmittance (b) of GQDs/PVA composite-based films prepared at different GQDs concentrations of 0, 5, 10, 15, and 20 wt%.

Figure 5(a) shows the UV-vis transmittance spectra of GQDs/PVA composite-based films prepared at different GQDs concentrations. It was found that GQDs/PVA composite-based films containing 5, 10, 15, and 20 wt% GQDs exhibited low UV transmittance excepted for PVA film (0 wt% GQDs) that still had high UV transmittance. Obviously, the GQDs/PVA composite-based film containing 20 wt% GQDs had minimum UV transmittance. This result implied that the GQDs caused a decrease in UV transmittance. Therefore, the average transmittance of GQDs/PVA composite-based films prepared at different GQDs concentrations is presented in Figure 5(b).

The average transmittances in UV and visible regions were analyzed under wavelength steps of 1 nm from 300 nm to 400 nm, and 400 nm to 740 nm, respectively. It seems that PVA film had the highest average UV transmittance of 91%, combined with 98% optical transparency under visible light, suggesting it was not capable of UV and visible shielding. In the case of GQDs/PVA composite-based films, the average UV transmittance decreased from 25% to 9.8% by increasing of the GQDs concentration, and their average UV transmittance was inversely proportional to the amount of the GQDs. Particularly, the GQDs/PVA composite-based film containing 20 wt% GQDs exhibited a UV transmittance of 9.8% (UV-shielding capacity of 90.2%), combined with 84% optical transparency under visible light and remained transparent to visible light. However, the average visible transmittance decreased from 98% to 85% by elevating the GQDs concentration because of higher GQDs content. This is in good agreement with a previous report [17] that the optical transparence in visible region is still higher than 80%. These results suggested that the GQDs played an important role in UV-shielding by considering the effect of UV absorption of GQDs, and remain transparent to visible light.

The absorption coefficient of UV-shielding film based on GQDs/PVA composite prepared at different GQDs concentrations is shown in Figure 6. It has seen that GQDs/PVA composite-based films containing 5, 10, 15, and 20 wt% GQDs exhibited a high absorption coefficient excepted for PVA film (0 wt% GQDs) that had the lowest absorption coefficient. Besides, the absorption coefficient in the UV range increased with increasing of the GQDs concentration and their absorption coefficient was directly proportional to the amount of the GQDs. Accordingly, these results implied that GQDs presented excellent properties for UV absorption.

In addition, contact angle measurement was performed to investigate the water-resistant behavior of GQDs/PVA composite-based films as shown in Figure 7. It seems that the PVA film (0 wt% GQDs) demonstrated a minimum contact angle in which abundant polar group (OH). For GQDs/PVA composite-based films, contact angle turned to high value and the maximum value was obtained for the 10 wt% GQDs, which benefited from a polar- polar interaction between GQDs and PVA to remain non-polar surface (hydrophobicity) of the composite film. This is in good agreement with a previous report [36] that a decrease in the number of -OH groups of PVA. Additionally, the evolution of the contact angle for a water drop versus time is shown in Figure 8. The time-dependent contact angle exhibited small change after contact with water for 60 s. The result indicated that the hydrophobic surface was improved for GQDs/PVA composite film with an appropriate mixture of GQDs and PVA. The high contact angle suggesting that the composite films can resist water interaction which may be a suitable coating material for long-time applications under a humidity environment.

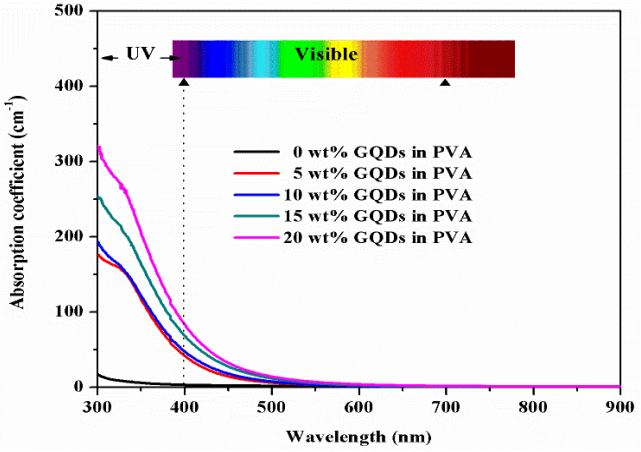

Figure 6. Plot of absorption coefficient versus wavelength for GQDs/PVA composite-based films prepared at different GQDs concentrations of 0, 5, 10, 15, and 20 wt%.

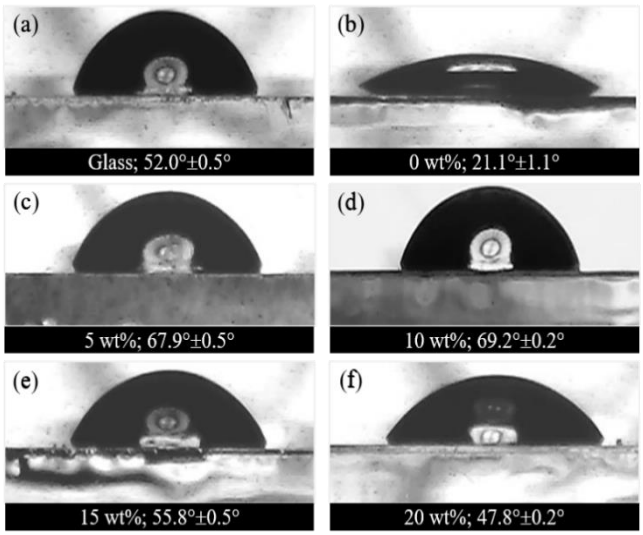

Figure 7. Contact angle of glass substrate (a), PVA film on glass substrate (b), and GQDs/PVA composite-based films prepared by using: 5 wt% GQDs (c), 10 wt% GQDs (d), 15 wt% GQDs (e), and 20 wt% GQDs (f).

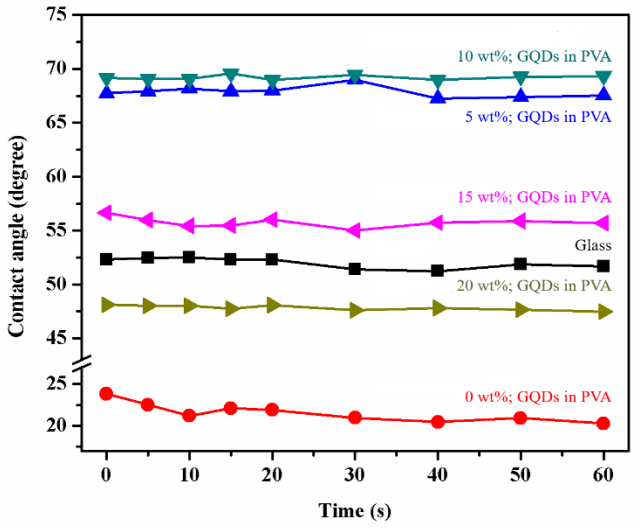

Figure 8. Evolution of the contact angle for a water drop versus time of glass and GQDs/PVA composite-based films for different GQDs concentrations.

As aforementioned, the decrease of UV transmittance showed the opposite trend with increasing the GQDs concentration (Figure 5(b)). This result suggested that UV transmittance could be decreased when the concentration was more than 20 wt%. In spite of superior UV-shielding characteristic, water resistance was reduced for the 20 wt% GQDs. This indicated that it could not be applied for waterproof packaging products. Accordingly, the GQDs/PVA composite-based film containing 10 wt% GQDs was an optimum condition for both UV-shielding and water resistance.

4. Conclusions

GQDs were successfully prepared by tuning the carbonization degree of the citric acid precursor. To fabricate UV-shielding films, GQDs/PVA composite gel was prepared by adding the GQDs into a transparent PVA gel at different concentrations of 0, 5, 10, 15, and 20 wt%. UV-shielding films were successfully prepared by screen printing of the GQDs/PVA composite gel on the glass substrate and sintering at 120°C overnight. The film thickness of approximately 60 µm was controlled by using one layer of tap spacer for all cases. Optical properties of UV-shielding film based on GQDs/PVA composites were investigated and compared to PVA films. It was found GQDs/PVA composite-based films offered an improved UV-shielding capacity when compared to PVA films. Particularly, the GQDs/PVA composite-based film containing 20 wt% GQDs exhibited a UV transmittance of 9.8 (UV-shielding capacity of 90.2%), combined with 84% optical transparency under visible light and remain transparent to visible light. For humidity environment application, the highest contact angle was explored for the 10 wt% GQDs contents suggesting sustainability for humidity environment application. Accordingly, GQDs played an important role in UV-shielding by considering the effect of UV absorption of the GQDs and the UV absorption of the GQDs can be explained in terms of the photon excitation by UV light. This GQDs/PVA composite could be potentially applied as transparent UV-protective coatings for pharmaceutical packing, food products packing, and UV-shielding or UV filter glass.

Acknowledgements

The authors acknowledge the Science Center Faculty of Science and Technology, Pibulsongkram Rajabhat University for providing measurement instruments. The authors wish to thank the Program of Physics, Faculty of Science and Technology, Pibulsongkram Rajabhat University and the Department of Physics, Faculty of Liberal Arts and Science, Kasetsart University Kamphaeng Saen Campus for providing supporting facilities.

References

[1] B.L. Diffey, "Sources and measurement of ultraviolet radiation," *Methods*, vol. 28, pp. 4-13, 2002.

[2] A.R. Young, J. Claveau and A.B. Rossi, "Ultraviolet radiation and the skin: Photobiology and sunscreen photoprotection," *Journal of the American Academy of Dermatology*, vol. 76, pp. S100-S109, 2017.

[3] S.C. Harrison, and W.F. Bergfeld, "Ultraviolet light and skin cancer in athletes," *Sports health*, vol. 1, pp. 335-340, 2009.

[4] I. Savoye, C.M. Olsen, D.C. Whiteman, A. Bijon, L. Wald, L. Dartois, F. Clavel-Chapelon, M.C. Boutron-Ruault and M. Kvaskoff, "Patterns of ultraviolet radiation exposure and skin cancer risk: The E3N-SunExp study," *Journal of epidemiology*, vol. 28(1), pp. 27-33, 2018.

[5] S.E. Duncan, and S. Hannah, "Light-protective packaging materials for foods and beverages," in *Emerging Food Packaging Technologies*, K.L. Yam and D.S. Lee, Eds., 1st ed., Cambridge, England: Woodhead Publishing, 2012, pp. 303-322.

[6] D.D. Shah, J. Zhang, H. Maity, and K.M.G. Mallela, "Effect of photo-degradation on the structure, stability, aggregation, and function of an IgG1 monoclonal antibody," *International Journal of Pharmaceutics*, vol. 547, pp. 438-449, 2018.

[7] J. Zhu, S. Yan, N. Feng, L. Ye, J.Y. Ou, and Q.H. Liu, "Near unity ultraviolet absorption in graphene without patterning," *Applied Physics Letters*, vol. 112, pp. 153106, 2018.

[8] P. Tian, L. Tang, K.S. Teng, and S.P. Lau, "Graphene quantum dots from chemistry to applications," *Materials Today Chemistry*, vol. 10, pp. 221-258, 2018.

[9] N.F. Attia, J. Park, and H. Oh, "Facile tool for green synthesis of graphene sheets and their smart free-standing UV protective film," *Applied Surface Science*, vol. 458, pp. 425-430, 2018.

[10] S. Xie, J. Zhao, B. Zhang, Z. Wang, H. Ma, C. Yu, M. Yu, L. Li, and J. Li, "Graphene oxide transparent hybrid film and its ultraviolet shielding property," *ACS Applied Materials & Interfaces*, vol. 7, pp. 17558-17564, 2015.

[11] Y. Dong, J. Shao, C. Chen, H. Li, R. Wang, Y. Chi, X. Lin, and G. Chen, "Blue luminescent graphene quantum dots and graphene oxide prepared by tuning the carbonization degree of citric acid," *Carbon*, vol. 50(12), pp. 4738-4743, 2012.

[12] P. Pimpang, R. Sumang, and S. Choopun, "Effect of concentration of citric acid on size and optical properties of fluorescence graphene quantum dots prepared by tuning carbonization degree," *Chiang Mai Journal of Science*, vol. 45(5), pp. 2005-2014, 2018.

[13] G. Eda, G. Fanchini, and M. Chhowalla, "Large-area ultrathin films of reduced graphene oxide as a transparent and flexible electronic material," *Nature Nanotechnology*, vol. 3, pp. 270-274, 2008.

[14] K.S. Kim, Y. Zhao, H. Jang, S.Y. Lee, J.M. Kim, K.S. Kim, J.H. Ahn, P. Kim, J.Y. Choi, and B.H. Hong, "Large-scale pattern growth of graphene films for stretchable transparent electrodes," *Nature*, vol. 457, pp. 706-710, 2009.

[15] M.L. Tsai, W.C. Tu, L. Tang, T.C. Wei, W.R. Wei, S.P. Lau, L.J. Chen, and Jr.H. He, "Efficiency enhancement of silicon heterojunction solar cells via photon management using graphene quantum dot as downconverters," *Nano Letters*, vol. 16(1), pp. 309-313, 2016.

[16] S. Bak, D. Kim, and H. Lee, "Graphene quantum dots and their possible energy applications: A review," *Current Applied Physics*, vol. 16(9), pp. 1192-1201, 2016.

[17] Z. Xie, Q. Du, Y. Wu, X. Hao, and C. Liu, "Full-band UV shielding and highly daylight luminescent silane-functionalized graphene quantum dot nanofluids and their arbitrary polymerized hybrid gel glasses," *Journal of Materials Chemistry C*, vol. 4, pp. 9879-9886, 2016.

[18] C. Ge, and G. Devar, "Formation of Polyvinyl Alcohol film with graphene nanoplatelets and carbon black for electrostatic discharge protective packaging," *Journal of Electrostatics*, vol. 89, pp. 52-57, 2017.

[19] F.F. Hilmi, M.U. Wahit, N.A. Shukri, Z.Ghazali, and A.Z. Zanuri, "Physico-chemical properties of biodegradable films of polyvinyl alcohol/sago starch for food packaging," *Materials Today: Proceedings*, vol. 16(4), pp. 1819-1824, 2019.

[20] N. Jain, V.K. Singh, and S. Chauhan, "A review on mechanical and water absorption properties of polyvinyl alcohol based composites/films," *Journal of the Mechanical Behavior of Materials*, vol. 26(5-6), pp. 213-222, 2017.

[21] T. Pauporté, "Highly transparent zno/polyvinyl alcohol hybrid films with controlled crystallographic orientation growth," *Crystal Growth & Design*, vol. 7(11), pp. 2310-2315, 2007.

[22] A.A. Tager, A.A. Anikeyeva, L.V. Adamova, V.M. Andreyeva, T.A. Kuz'mina, and M.V. Tsilipotkina, "The effect of temperature on the water solubility of polyvinyl alcohol," *Polymer Science USSR*, vol. 13(3), pp. 751-758, 1971.

[23] M.H. Makled, E. Sheha, T.S. Shanap, and M.K. El-Mansy, "Electrical conduction and dielectric relaxation in p-type PVA/CuI polymer composite," *Journal of advanced research*, vol. 4(6), pp. 531-538, 2013.

[24] G.S. Kumar, U. Thupakula, P.K. Sarkar, and S. Acharya, "Easy extraction of water-soluble graphene quantum dots for light emitting diodes," *RSC Advances*, vol. 5(35), pp. 27711-27716, 2015.

[25] S. Ye, F. Xiao, Y.X. Pan, Y.Y. Ma, and Q.Y. Zhang, "Phosphors in phosphor-converted white light-emitting diodes: Recent advances in materials, techniques and properties," *Materials Science and Engineering: R: Reports*, vol. 71(1), pp. 1-34, 2010.

[26] P. Yang, L. Zhou, S. Zhang, N. Wan, W. Pan, and W. Shen, "Facile synthesis and photoluminescence mechanism of graphene quantum dots," *Journal of Applied Physics*, vol. 116(24), pp. 244306-1-7, 2014.

[27] J. Gu, X. Zhang, A. Pang, and J. Yang, "Facile synthesis and photoluminescence characteristics of blue-emitting nitrogen-doped graphene quantum dots," *Nanotechnology*, vol. 27(16), pp. 165704, 2016.

[28] H. Guo, F. Pang, X. Zeng, and T. Wang, "PbS quantum dot fiber amplifier based on a tapered SMF fiber," *Optics Communications*, vol. 285, pp. 3222-3227, 2012.

[29] D. Raeyani, S. Shojaei, S.A. Kandjani, and W. Wlodarski, "Synthesizing graphene quantum dots for gas sensing applications," *Procedia Engineering*, vol. 168, pp. 1312-1316, 2016.

[30] I.M. Jipa, A. Stoica, M. Stroescu, L. M. Dobre, T. Dobre, S. Jinga, and C. Tardei, "Potassium sorbate release from poly (vinyl alcohol)-bacterial cellulose films," *Chemical Papers*, vol. 66(2), pp. 138-143, 2012.

[31] Q. Luo, Y. Shan, X. Zuo, and J. Liu, "Anisotropic tough poly(vinyl alcohol)/graphene oxide nanocomposite hydrogels for potential biomedical applications," *RSC Advances*, vol. 8(24), pp. 13284-13291, 2018.

[32] G. Yang, X. Wan, Y. Liu, R. Li, Y. Su, X. Zeng, and J. Tang, "Luminescent poly(vinyl alcohol)/carbon quantum dots composites with tunable qater-induced shape memory behavior in different pH and temperature environments," *ACS Applied Materials & Interfaces*, vol. 8(50), pp. 34744-34754, 2016.

[33] T. Cheng-an, Z. Hao, W. Fang, Z. Hui, Z. Xiaorong, and W. Jianfang, "Mechanical properties of graphene oxide/polyvinyl alcohol composite film," *Polymers and Polymer Composites*, vol. 25(1), pp. 11-16, 2017.

[34] T. Wang, Y. Li, S. Geng, C. Zhou, X. Jia, F. Yang, L. Zhang, X. Ren, and H. Yang, "Preparation of flexible reduced graphene oxide/poly(vinyl alcohol) film with superior microwave absorption properties," *RSC Advances*, vol. 5(108), pp. 88958-88964, 2015.

[35] X. Yang, Y. Li, Q. Du, X. Wang, S. Hu, L. Chen, Z. Wang, Y. Xia, and L. Xia, "Adsorption of methylene Bblue from aqueous solutions by polyvinyl alcohol/graphene oxide composites," *Journal of Nanoscience and Nanotechnology*, vol. 16(2), pp. 1775-1782, 2016.

[36] P. Chouwatat, P. Polsana, P. Noknoi, K. Siralertmukul, and K. Srikulkit, "Preparation of hydrophobic chitosan using complexation method for PLA/Chitosan blend," *Journal of Metals, Materials and Minerals*, vol. 20(1), pp. 41-44, 2010.